



An engineering vision about composite sandwich structures analysis

Francisco K. Arakaki¹ · Alfredo Rocha de Faria²

Received: 30 January 2018 / Accepted: 5 May 2018 / Published online: 6 June 2018
© The Brazilian Society of Mechanical Sciences and Engineering 2018

Abstract

As shown in the literature, there is plentiful information about sandwich panels. Two of the most common points under discussion are the failure modes and the efficiency of numerical simulations considering the stiffness and interlaminar stress. The failure modes in the literature are not always likely to happen in practice, and representing them becomes a challenging task. Regarding the numerical simulations, new assumptions and formulations appear in order to consider the shear stress in the honeycomb CORE and to minimize processing time in 3D models. Although new mathematical solutions emerge, in some cases they are unpractical for engineering applications and must be evaluated and compared with test results in order to verify their consistency. Therefore, experimental results are necessary to validate theories to comply with the failure modes observed in sandwich panels and to validate the finite element model. Also, the main focus of the literature is on the theoretical formulation and not in engineering applications. In this sense, the main contribution of this paper is to bring forward experimental results of aeronautical sandwich panels whose data are scarce and therefore contributes to the validation of new developments. In addition, the purpose of this work contributes to the use of the finite element models with composite sandwich panels where the appropriate input for 2D (plate) and 3D (solid) elements is unclear. It should be pointed out that for failure investigation the first step is validating the finite element model. In this sense, a typical aircraft panel with experimental results is presented. The finite element model and the input parameters that are not mentioned in the classical literature are also presented. The experimental strain from specimen tested agreed well with the numerical simulations results.

Keywords Composite materials · Sandwich panel · Finite element analysis · Panel test · Classical theory

1 Introduction

In the NASA report, Poland [1] describes a case study for a commercial Boeing airplane with diameter ranging from 244 to 398 inch presenting similar characteristics of an airplane 80% of the Boeing 747 size. Cost and weight reduction was the purpose of this study, and a similar aluminum structure was used as baseline. Two concepts were studied: the B family with skin and frames mechanically attached and skin and stiffeners co-cured, and the D

family with a sandwich structure with co-bonded circumferential frames. In many aspects the sandwich structure showed better results compared to the others with respect to cost, probability of success (manufacturing and structural performance) and weight saving.

Matsui [2] describes the proof of concept development for the executive jet Honda-Jet. Similar to the work of Poland [1], the results showed weight and cost saving with sandwich panels construction when compared to conventional aluminum alloys.

In Kupke and Kolax [3], an ambitious project with 30% weight reduction and 40% cost reduction, when compared with the aluminum fuselage A320 airplane, was carried out. Ease in maintenance and improvement of passengers comfort were also the purpose of this study. After evaluating several design concepts, two different concepts were highlighted: (a) the Vesco (Ventable Shear Core) and (b) SoFi (Stringer outside Frames inside). Vesco is a special type of sandwich, as shown in Fig. 1. Vesco is not symmetrical, with the internal skin supporting more load

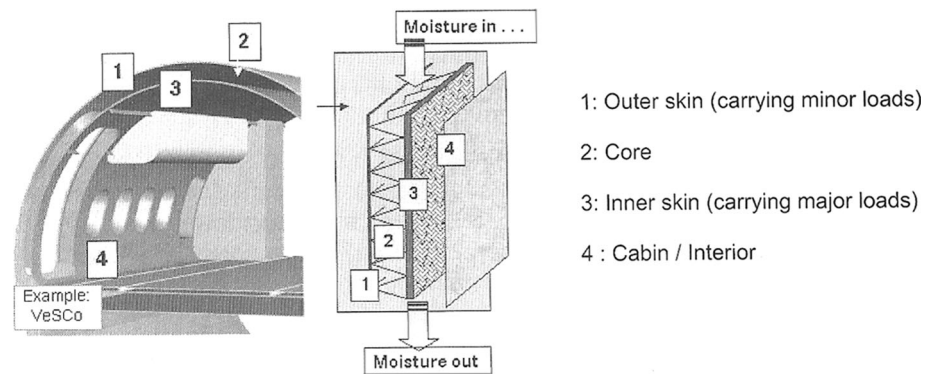
Technical Editor: André Cavalieri.

✉ Francisco K. Arakaki
francisco.arakaki@embraer.com.br

¹ EMBRAER S.A., Av. Brigadeiro Faria Lima, 2170, Putim, São José dos Campos 12227-901, Brazil

² Instituto Tecnológico de Aeronáutica (ITA), São José dos Campos, SP, Brazil

Fig. 1 VeSCo (Ventable Shear Core) concept—Kupke and Kolax [3]



than the outside skin. The core material is designed to prevent moisture accumulation, which is a risk for the practical application of sandwich panels.

In July 2013, the CMH17 “Composite Materials Handbook” [4] in Rev. G published Chapter 6, “Structural Sandwich Composites” with several topics including “Design and Analysis of Sandwich Structures.” In this chapter, a section on “Finite Element Modeling of Sandwich Structure” is included. In December 2014, the CMH17 presented yet another review on the subject.

The uses of aeronautical sandwich panels in the Embraer airplane Legacy 500 are shown in Fig. 2. The applications of the sandwich panels in this airplane are wing composite shroud, flap track fairing, wing-to-fuselage fairing (Fig. 2a), tail cone (Fig. 2b), tail boom (Fig. 2c), scoop, horizontal empennage fairing, spoiler, wing stub upper skin, forward fuselage pressure bulkhead and nose landing gear bay upper cover.

Over time the application of composite sandwich panels has been growing and nowadays the subject requires further investigation. Numerous references about and aspects of sandwich structures application are well discussed by Vinson [5] with respect to past, present and future. This work cites the first research paper (1944) concerning sandwich construction up to 1999, when the Journal of Sandwich Structures and Materials was launched.

Recently Caliri et al. [6] presented a review on plate and shell theories for laminated and sandwich structures

highlighting the finite element method. In this work a review about 100 papers was done describing the stage for new theories and solution methods for laminated and sandwich structures.

In summary, the investigation about sandwich structures can be divided in three categories: (1) laminate plate theory with mathematical approach considering the kinematic behavior, (2) new finite element development and (3) theoretical versus experimental investigation described in the following papers.

D’Ottavio et al. [7], based on the principle of virtual displacements and the method of Ritz, derived the governing equations for composite bending analysis and sandwich structures. In this paper, many references are cited regarding sandwich plate theory. One interesting point is that a number of test cases from the literature were discussed, and results were validated against exact 3D solutions.

Linke et al. [8], using a displacement-based finite element, perform static and stability analyses of sandwich plates considering the three-layer sandwich model. In this work, the face sheets are idealized as classical plate elements assuming the Kirchhoff–Love hypothesis. One interesting remark that agrees with industrial needs is the necessity for fast finite elements for sandwich structures accounting for the nonlinear deformation pattern in low-strength cores and a very high computational effort not

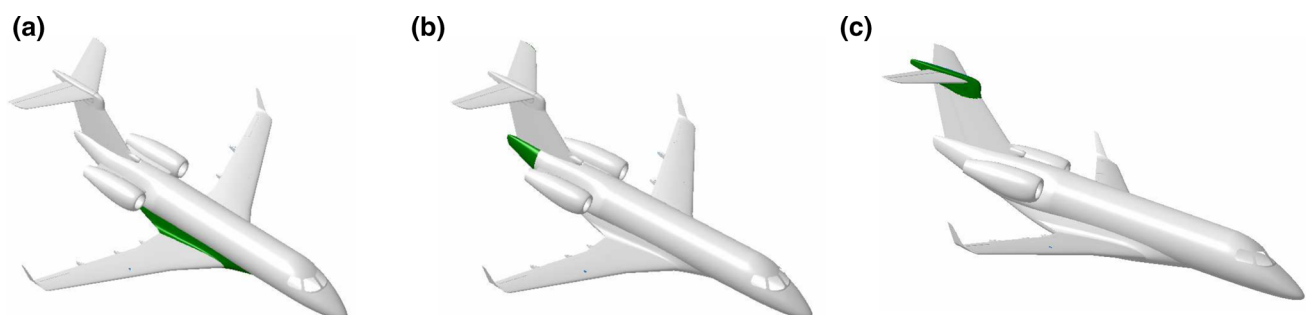


Fig. 2 Examples of aeronautical sandwich panels applications. **a** Wing to fuselage. **b** Tail cone. **c** Tail boom

only during the design of large sandwich structures but also in early design stages.

One interesting investigation was conducted by Wahl et al. [9]. This work addresses an utmost relevant point for engineers: the search for analytical solutions easy to apply and that comply conservatively with test results. Also, the free-of-solid elements FEM (finite element model) proposed opens up new possibilities for analysis methodology.

In summary, pragmatic investigations must be able to provide a theory that complies with experimental results. Although there are theories emerging, they must be validated and their applicability in real problems must be checked.

One important issue concerning the use of the 3D element is the material behavior. In Bompan [10], the geometry of the core is analyzed separately to understand the behavior and then the core allowable is introduced in the global model through the material properties cards.

Therefore, due to the growing interest in this subject, the main objective of this paper is to address aeronautical composite sandwich panel experimental results and their respective finite element modeling since essential input data details are not showed in most, if not all, works previously published.

2 Classical literature

The main features about sandwich classical failure aspects are well addressed in two classical references for industrial applications: Bruhn [11], about formulation, and HyperSizer [12], about analysis tools. Additional literature references are Allen [13], Burton [14], Noor [15] and Bitzer [16].

HEXCEL [17] shows the laminate sandwich use advantages compared with a solid laminate of thickness t . There is great stiffness gain with a small increase in weight. In this reference, there are several other data including mechanical properties data.

Another information to be highlighted is about the sandwich panel's allowable strength. Usually they are tested with 0.65 inch thicknesses for aluminum core and with 0.50 inch for nonmetallic core. Therefore, in Niu [18], the honeycomb thickness versus correction factor to be applied to sandwich panels with different thicknesses as specified in the manufacturer test must be applied.

Bruhn [11] shows the most common failure modes in sandwich structures. In CMH17 [4], it is observed that more failure modes were included. Both references mention the mathematical formulations involved in each failure mode, although in some cases they are not likely to be observed in practice. In this sense, the failure mode wrinkle face (core separation) was studied in Widmaier and

Arakaki [19] with the purpose of reproducing this failure mode. It should be pointed out the contribution of the ESDU [20], in particular ESDU 81047 [21], 87013 [22] and 88015 [23], in the analysis by classical formulations.

Considering the commercial software that addresses some of the presented failure modes, it is noted that HyperSizer [12] software is customized to examine: (a) sandwich shear crimping failure criteria, (b) sandwich core crushing failure criteria, (c) sandwich intracell dimpling failure criteria, (d) sandwich analysis in general, (e) sandwich shear strength failure criteria and (f) sandwich facesheet wrinkling failure criteria.

In order to apply the classical theory formulation, the problem must be well defined. One example is the sandwich panel facesheet wrinkling analysis described in HyperSizer [24]. In accordance with HyperSizer documentation, for honeycomb cores, Eq. (1) is proposed based on the Ley [25] and Hexcel [26] references.

$$\sigma_{wr} = k_2 E_f \sqrt{\frac{E_c t_f}{E_f t_c}} \quad (1)$$

where σ_{wr} is the wrinkling stress allowable, E_f is the elastic modulus of facesheet, E_c is the through-the-thickness elastic modulus of core, t_f is the facesheet thickness, t_c is the core thickness, k_2 is related to the core type, and the physical interpretation of this coefficient refers to the boundary condition imposed by core in the skin behavior related to facesheet wrinkling.

Ley [25] suggests a wrinkling factor to use with the wrinkling allowable stress equation, which is $k_2 = 0.82$, that is derived from the physics of sandwich facesheet wrinkling and Eq. (2) for the elastic modulus of facesheet, E_f , in case of composite materials.

$$E_f = \frac{12D_{11}}{t_f^3} \quad (2)$$

HyperSizer computes the term D_{ij} , equivalent flexural modulus, using D_{11} term from the 3×3 \mathbf{D} matrix of the classical lamination theory. Also, in the HyperSizer reference, the analyses do not include the effect of adhesive layer, and the wrinkling stress of sandwich panels with very thin facesheets is likely overly conservative. In accordance with Gutierrez [27], the effect of a 0.005"-thick adhesive layer on the theoretical wrinkling stress of a 0.010"-thick facesheet on a 1.0"-thick core increases wrinkling stress by 50%.

Therefore, due to the difficulty to analyze some unconventional problems by classical literature and to validate test data in cases where more detail is necessary as mentioned in the HyperSizer documentation, the finite element method complements the analysis. So, the next topic is dedicated to the finite element method, implemented in NASTRAN software [28].

3 Finite element method

In CMH-17 [4], Volume 6, Rev. G, Chapter 4, section (4.12) is dedicated to the finite element method. It is mentioned the care that must be taken when analyzing sandwich structures with the finite element method. The main concern is about shear deformation of the core that must be taken into account in some problems. Whether it is considered or not can lead to non-conservative results for the eigenvalues determination in buckling behavior. So, the correct choice of the finite element is fundamental in such cases. Another remark is made about the use of 3D elements with respect to the transverse stresses that are not taken into account in shell elements. This consideration is important for core strength. Regarding modeling the CMH-17 highlights: (a) the global model, (b) the model of layers and (c) the solid model.

In the global model, the structure is represented by a single plate element with equivalent properties. The main reason for this simplification is to obtain the element forces for further analysis. In the layers model, the structure is divided into three or more layers. In this model, according CMH17, all layers have a common, unique rotation through the cross section of the sandwich. Because the core material generally only offers shear stiffness, shear-flexible shell elements are typically used in layered shell models. Shell elements based on the classical Kirchhoff–Love theory can be used; however, such an approach ignores the transverse shear flexibility offered by the sandwich structure.

In the solid model, the structure can be represented by shell elements for skin and solid elements to the core. The discretization of the core depends on the degree of information desirable about the transverse shear deformation. In this model, the displacement field compatibility between shell and solid elements must be considered during the modeling process. In accordance with CMH-17, this may be achieved by defining an offset between the centerline of the skin surfaces and the nodes, which are at the corners of the solid elements. In the full solid model, the skin and the core are modeled as 3D elements. Due to the computational cost, this type of analysis is used when a detailed local analysis is required.

It is common to use the card PSHELL in many cases in the finite element model. Then, according to the Loughlin [29], the following observations on the fields of PSHELL card are proposed:

- (a) the term (MiD1, T) refers to in-plane load of a honeycomb panel. Assuming that the face is responsible for the loads in the plane, then MiD1 refers to the face material, and T is the total thickness of the faces [$T = (t/2)$ superior + $(t/2)$ inferior], see Fig. 3;

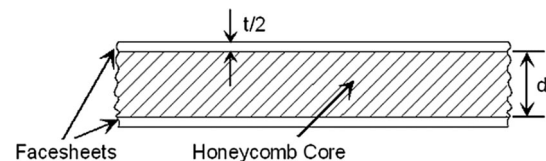


Fig. 3 Sandwich structure nomenclature [16]

- (b) (MID2, $12*I/T3$) refers to bending load of the honeycomb panel. Assuming that the face is also responsible for bending, MiD2 refers to the material face, and $12*I/T3$ is the inertia of a rectangular plate, considering:
- (b.1) for thin facesheets and a thick core, “ I ” for Honeycomb is approximately $T * d^2/4$;
- (b.2) for facesheets thicker relative to the core, then “ I ” is $[2/3][(d/2) + (T/2)]^3 - [d^3/12]$;
- (c) (MiD3, TS/T) refers to shear load of the honeycomb panel. Assuming that all the core is responsible for shear, then MiD3 refers to material of the core, TS is the thickness of the core, “ d ” in Fig. 3, and T is the total thickness of the faces;
- (d) (NSM) refers to non-structural mass. The density “rho” is ignored in the MiD3 card; however, the mass of the core material and the adhesive must be included. Then NSM is mass per unit area and is determined by (“rho” nominal) * (d).

Nabarrete [30] presents a study of three-layer finite element. In this model, the sandwich panel faces are represented by Reissner–Mindlin plates, while the core is modeled as a continuous three-dimensional element. This model allows representing with good accuracy, a variety of core types and stiffness. The three-dimensional problem is reduced to two dimensions by the analytical integration of energy through the thickness to obtain the mass and stiffness matrices. This leads to computational efficiency. Compared to the solid model, this theory avoids numerical problems present in the three-dimensional models with aspect ratios not recommended in practice.

Although numerous works have been published there is a difficult of the users about finite element application to understand the composite sandwich structures application. In practice the Nastran cards input is at the heart of these difficulties. Therefore, the results of the finite element method highlighting Nastran card inputs are shown in the application section.

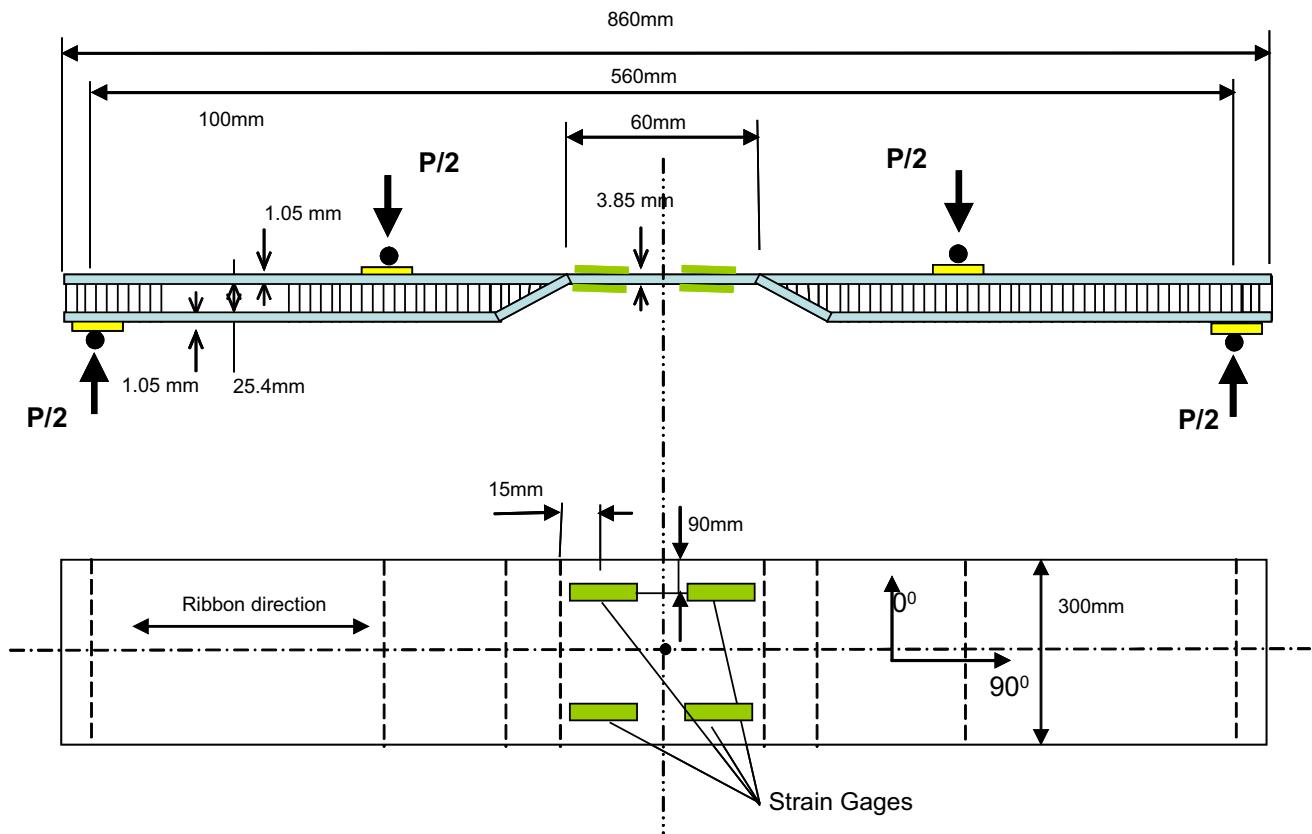


Fig. 4 Typical sandwich panel

4 Application

The typical sandwich panel shown in Fig. 4 was chosen for study where the solid laminate represents the attachment region and the full-thickness structural honeycomb represents the region where high bending stiffness is required. The specimen is representative for the purposes it is designed to since the manufacturer process is certified. The purpose of this application is to show and discuss the parameters involved in finite element structural analysis and the use of classical analysis with the approach used.

The test fixture to represent the conditions shown in Fig. 4 is described in Fig. 5a–c. As shown in Fig. 5a, the four-point bending condition was used. The support and loading span were adjusted to reach the target strain for the test. In Fig. 5b, a detail about the point of load application is shown. As noted roller and chamfer were used to fit the rotation between the skin plane with the base plane of the load application point. In Fig. 5c, strain gages back to back, symmetric with center line and symmetric with longitudinal line, in four points were used to verify the load distribution and to check the numerical and experimental results. In this study, the displacement was not the primary concern because in the airplane certification proposal

usually the strains are used to show no damage growth behavior.

The presence of a ramp in this structure justifies the use of shell/solid model. The complete model is shown in Fig. 6a with details in load application point and boundary conditions used. Observe that the boundary condition “1” was introduced to avoid the rigid body motion. This model was built using CQUAD4 plate element and solid element CHEXA with eight nodes and CPENTA with six nodes, as shown in Fig. 6b. Details about these elements are shown in Nastran [28]. The full model has 29,888 elements and 20,599 nodes. Since a good agreement between the theoretical and experimental results was reached (see Fig. 14), it was concluded that the finite element mesh is adequate. The face sheets material is carbon fabric/epoxy, and core material is Nomex Honeycomb HRH10-1/8-4.0,1.0IN. Figure 6c shows the interface between face sheet elements and core elements, which was assumed to have the same nodes. The adhesive is not being considered in this model. Observe that, in this analysis, the thickness of the core was modeled with just one solid element through the thickness.

The mechanical properties of Nomex Honeycomb can be found in the manufacturer’s catalogs, and considering the Hexcel reference, the properties of HRH10-1/8-

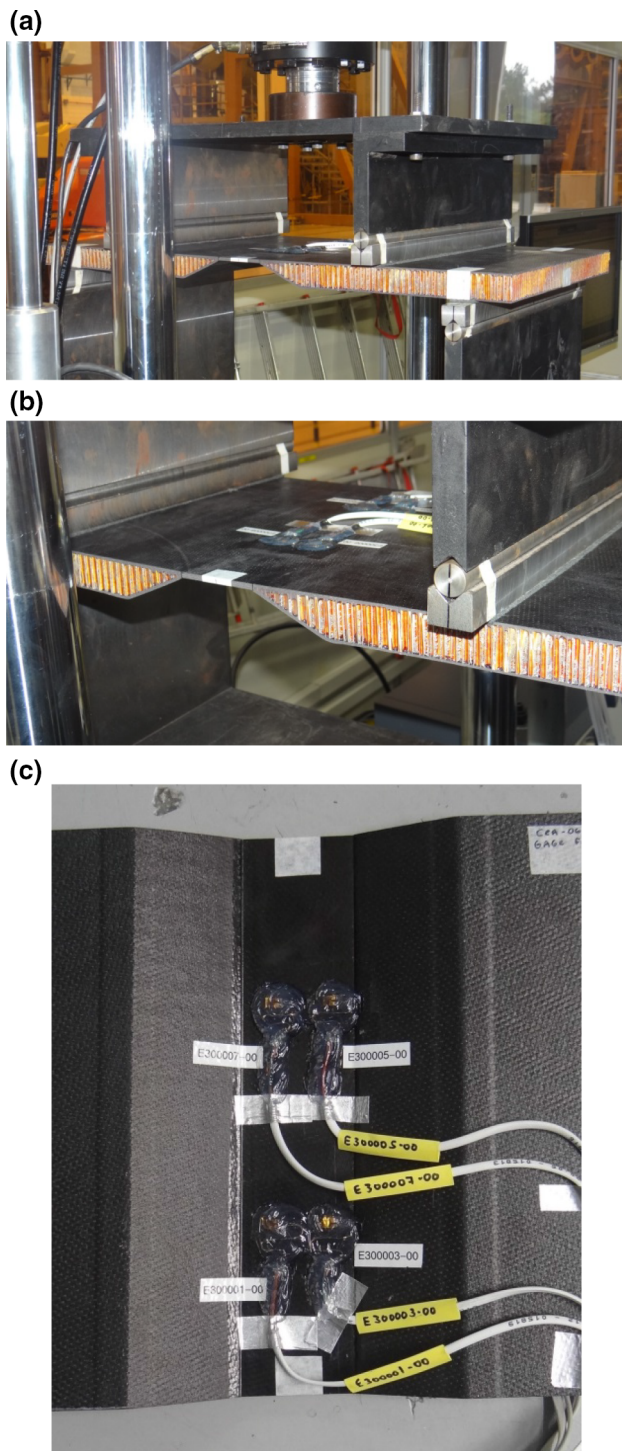


Fig. 5 a Test setup general view—Langellotti [31]. b Test setup detail view—load application points. c Instrumentation detail view—strain gages back to back

4.0,0.5IN are shown in Table 1 and the mechanical properties of carbon fabric/epoxy are shown in Table 2.

The details of stacking sequence are shown in Fig. 7. The PCOMPG card for skin elements and MAT9 card (defines the material properties for linear, temperature-

independent, anisotropic materials for solid isoparametric elements) for solid elements were used to have more flexibility in the assignment of mechanical properties of the core.

An illustration of a PCOMPG card (defines global ply IDs and properties for a composite material laminate) is shown in Fig. 8 only for the solid laminate and the honeycomb region. The data relating to MAT9 card are shown in Eq. 3. Note that, in Eq. (3), we are assuming uncoupled behavior, for shear stress and minimum coupled behavior for stress in the plane 1–3. Three values in the principal diagonal come from Table 1 (elastic modulus) and the others were assumed to be very small in order to reflect the sandwich structural behavior. Figure 9 shows the planes relating the material properties.

$$\begin{Bmatrix} \sigma_x \\ \sigma_y \\ \sigma_z \\ \tau_{xy} \\ \tau_{yz} \\ \tau_{zx} \end{Bmatrix} = \begin{bmatrix} C_{11} & C_{12} & C_{13} & C_{14} & C_{15} & C_{16} \\ & C_{22} & C_{23} & C_{24} & C_{25} & C_{26} \\ & & C_{33} & C_{34} & C_{35} & C_{36} \\ & & & C_{44} & C_{45} & C_{46} \\ & & & & C_{55} & C_{56} \\ & & & & & C_{66} \end{bmatrix} \begin{Bmatrix} \varepsilon_x \\ \varepsilon_y \\ \varepsilon_z \\ \gamma_{xy} \\ \gamma_{yz} \\ \gamma_{zx} \end{Bmatrix}; \tag{3}$$

$$\begin{Bmatrix} \sigma_x \\ \sigma_y \\ \sigma_z \\ \tau_{xy} \\ \tau_{yz} \\ \tau_{zx} \end{Bmatrix} = \begin{bmatrix} 0.01 & 0 & 0.01 & 0 & 0 & 0 \\ & 0 & 0.01 & 0.01 & 0 & 0 & 0 \\ & 0.01 & 0.01 & 193 & 0 & 0 & 0 \\ & 0 & 0 & 0 & 0.01 & 0 & 0 \\ & 0 & 0 & 0 & 0 & 32 & 0 \\ & 0 & 0 & 0 & 0 & 0 & 59 \end{bmatrix} \begin{Bmatrix} \varepsilon_x \\ \varepsilon_y \\ \varepsilon_z \\ \gamma_{xy} \\ \gamma_{yz} \\ \gamma_{zx} \end{Bmatrix}$$

In this typical sandwich panel Eq. (1) was used to show one application using the classical analysis. Therefore, wrinkling stress in the upper skin was used to verify the stress allowable in constant thickness region. Considering the material properties shown in Table 3, and using the classical lamination theory, the value of D_{11} term from the 3×3 D matrix can be obtained.

5 Results

Based on the boundary conditions and the maximum applied load (2556 N), the following results considering linear analysis can be obtained. The loading applied corresponds to the load required to reach our goal strain. Figure 10 shows the numerical displacement behavior. Figure 11 shows the failure index assuming Tsai-Wu criteria only for plate elements. Assuming linear behavior, the failure load is 5112 N, considering FPF (first-ply failure) criteria. Figure 12 shows the longitudinal compression strain (0° ply) in the first ply of the upper skin, and Fig. 13 shows the shear stress for the solid elements.

Fig. 6 **a** Finite element model—loading and boundary conditions. **b** FEM—plate and solid elements. **c** FEM—interface between facesheet and core element

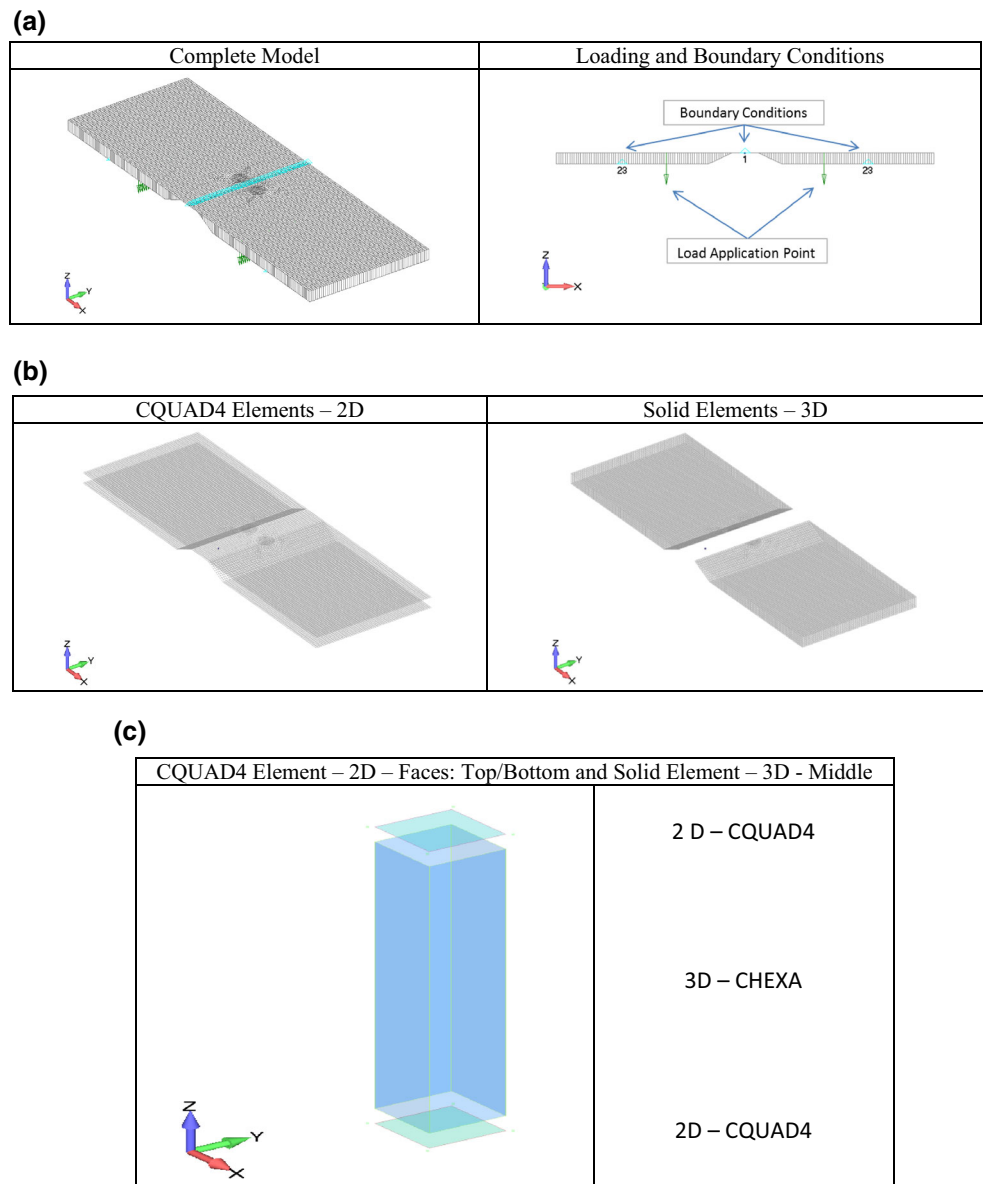


Table 1 Mechanical properties—“Hexcel” @ ambient temperature

Hexcel honeycomb designation: material–cell–density	Compressive					Plate shear					
	Bare		Stabilized			L direction			W Direction		
	Strength (MPa)	Modulus (MPa)	Strength (MPa)	Modulus (MPa)	Strength (MPa)	Modulus (MPa)	Strength (MPa)	Modulus (MPa)	Strength (MPa)	Modulus (MPa)	
Hexagonal	typ	min	typ	min	typ	typ	min	typ	typ	min	typ
HRH-10-1/8-4.0	3.59	2.76	3.96	3.24	193.05	1.76	1.55	59.29	0.97	0.79	32.41

Test data obtained at 0.50 inch thickness

In Fig. 5c strain gage back to back to measure the deformations is shown. Considering the average strain values, in Fig. 14, the experimental results correlated very

well with finite element method results, discussed in the previous section. The physical interpretation of the strain was confirmed by two strain gages located in the lower and

Table 2 Mechanical properties—fabric carbon/epoxy

Fabric—carbon/Epoxi									
E_1 (MPa)	E_2 (MPa)	G_{12} (MPa)	ν_{12}	X_T (MPa)	Y_T (MPa)	X_C (MPa)	Y_C (MPa)	S_{12} (MPa)	
71,350	62,601	4598	0.09	678	645	548	536	122	

Fig. 7 Auxiliary data—PCOMPG card and stacking sequence



Monolithic Laminate		Ramp		Honeycomb	
A2 (0,90)	A3 (±45)	A4 (0,90)	A5 (±45)	A6 (0,90)	A7 (±45)
A3 (±45)	A4 (0,90)	A5 (±45)	A6 (0,90)	A7 (±45)	A8 (0,90)
A4 (0,90)	A5 (±45)	A6 (0,90)	A7 (±45)	A8 (0,90)	A9 (±45)
A5 (±45)	A6 (0,90)	A7 (±45)	A8 (0,90)	A9 (±45)	A10 (0,90)
A6 (0,90)	A7 (±45)	A8 (0,90)	A9 (±45)	A10 (0,90)	A11 (±45)
A7 (±45)	A8 (0,90)	A9 (±45)	A10 (0,90)	A11 (±45)	A12 (0,90)
A8 (0,90)	A9 (±45)	A10 (0,90)	A11 (±45)	A12 (0,90)	Core
A9 (±45)	A10 (0,90)	A11 (±45)	A12 (0,90)	Core	Core
A10 (0,90)	A11 (±45)	A12 (0,90)	Core	Core	Core
A11 (±45)	A12 (0,90)	Core	Core	Core	Core
A12 (0,90)	Core	Core	Core	Core	Core

Solid Laminate Region						Core Region					
PCOMPG	1200280	69.	TSAI			PCOMPG	1200282	69.	TSAI		
2	15022	0,35	0	YES		2	15022	0,35	0	YES	CQUAD4
3	15022	0,35	45	YES		3	15022	0,35	45	YES	for upper skin
4	15022	0,35	0	YES		6	15022	0,35	0	YES	
5	15022	0,35	45	YES		MAT 9					
6	15022	0,35	0	YES		CHEXA					
7	15022	0,35	45	YES		for core					
8	15022	0,35	0	YES		PCOMPG	1200283	69.	TSAI		
9	15022	0,35	45	YES		8	15022	0,35	0	YES	CQUAD4
10	15022	0,35	0	YES		11	15022	0,35	45	YES	for lower skin
11	15022	0,35	45	YES		12	15022	0,35	0	YES	
12	15022	0,35	0	YES							

Fig. 8 PCOMPG card

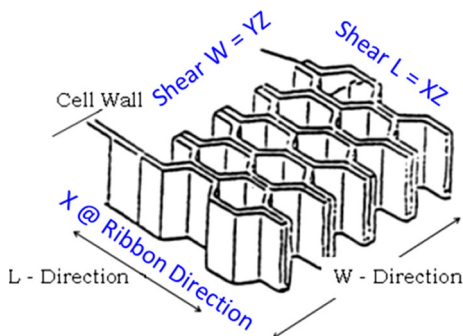


Fig. 9 Honeycomb material properties planes

upper faces. Upper face is in compression, and lower face is in tension behavior. The maximum percentage error between the experimental and numerical was 12.4%. It should be pointed out that the deformations are in solid laminate, pure bending region, but very near the ramp termination.

Considering the classical theory application in the upper skin, Table 3 summarizes the results for wrinkling stress allowable according the Eq. (1).

The wrinkling stress allowable shown in Table 3 is slightly higher than the longitudinal compression material allowable presented in Table 2 (X_C). Therefore, the panel is prone to failure in compression strength, whereas wrinkling

Table 3 Wrinkling stress allowable by classical theory

k_2	Wrinkling stress allowable @ classical analysis					
	D_{11}^{-1} (1/N mm)	E_f (MPa)	E_c (MPa)	t_f (mm)	t_c (mm)	σ_{wr} (MPa)
0.82	1.48E-04	69,968	193	1.05	25.4	613

Fig. 10 Linear—numerical displacement (mm) behavior

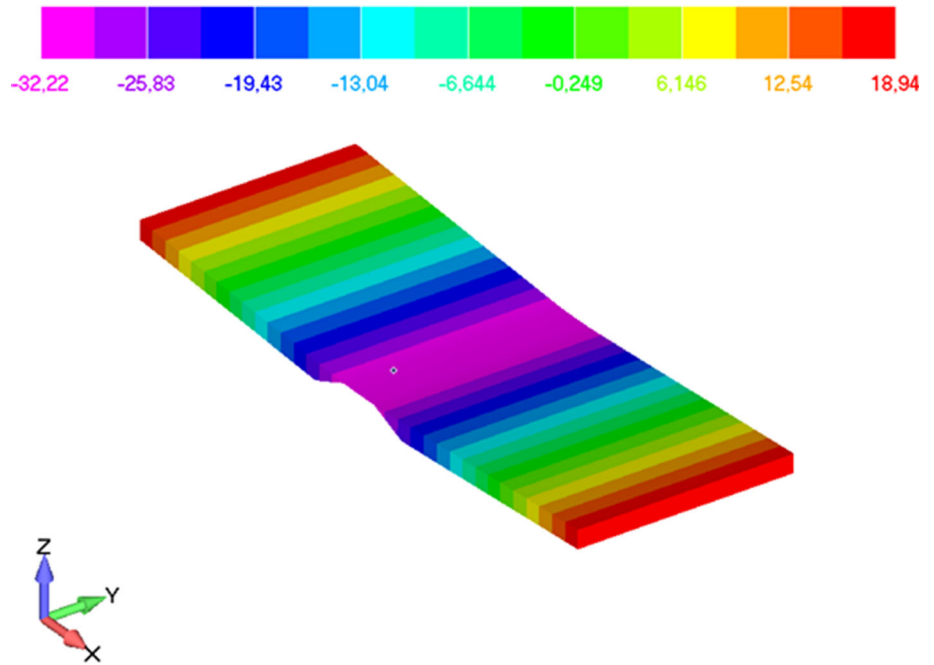
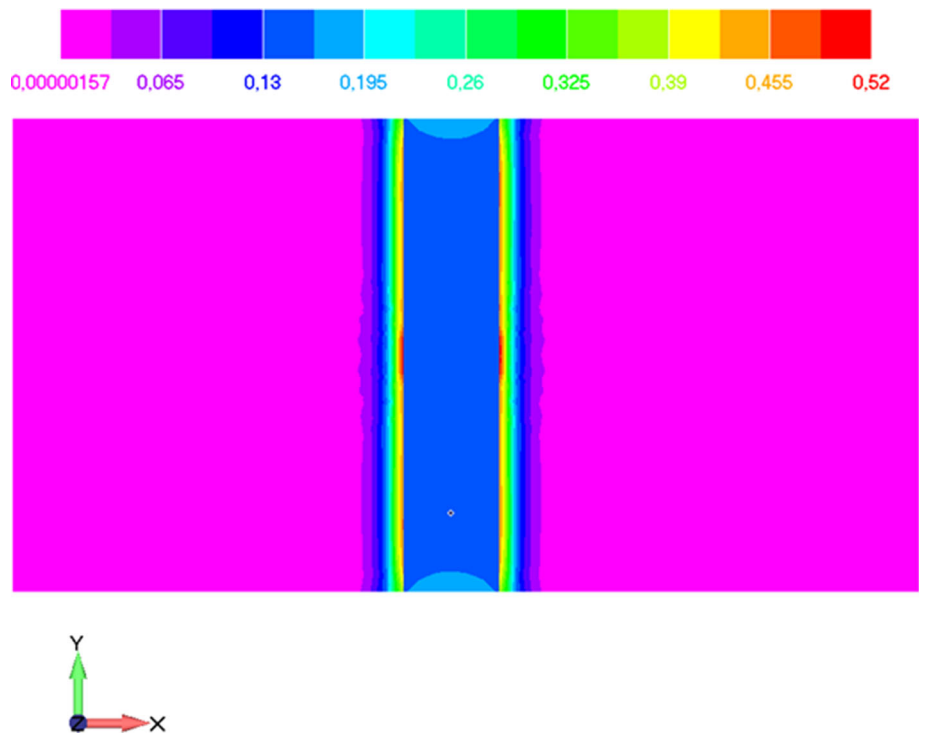


Fig. 11 Linear—numerical failure index—Tsai-Wu



in the upper skin is unlikely to happen. Also, considering the wrinkling stress allowable, and assuming the effective elastic modulus of the facesheet, the wrinkling strain

allowable is 10,593 μ -strain, which is very high when compared to Fig. 14. This result leads to the conclusion that wrinkling in the upper skin is unlikely to happen.

Fig. 12 Linear—longitudinal compression strain (mm/mm)

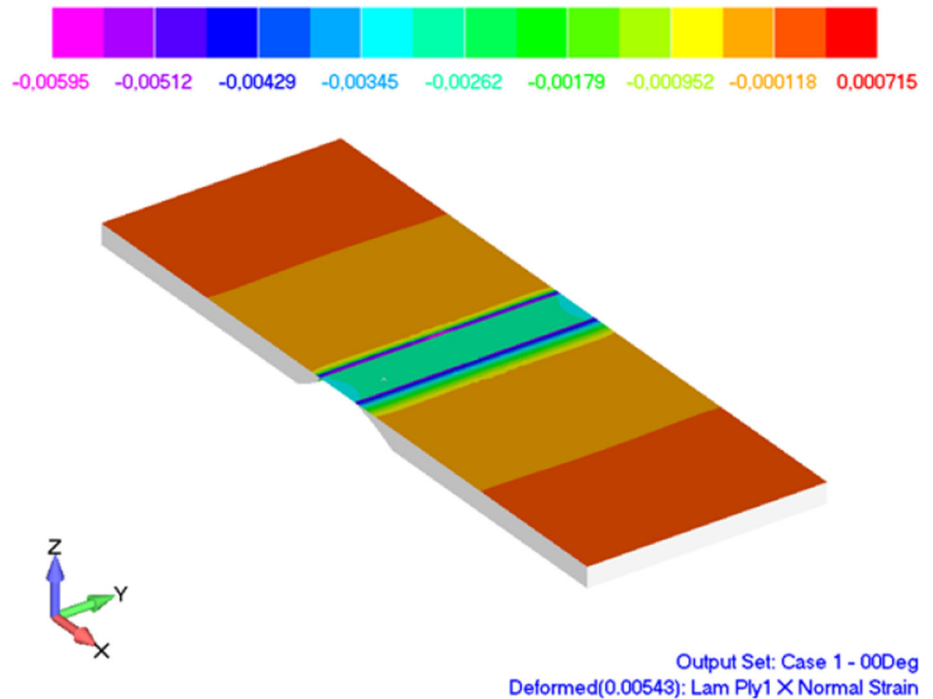
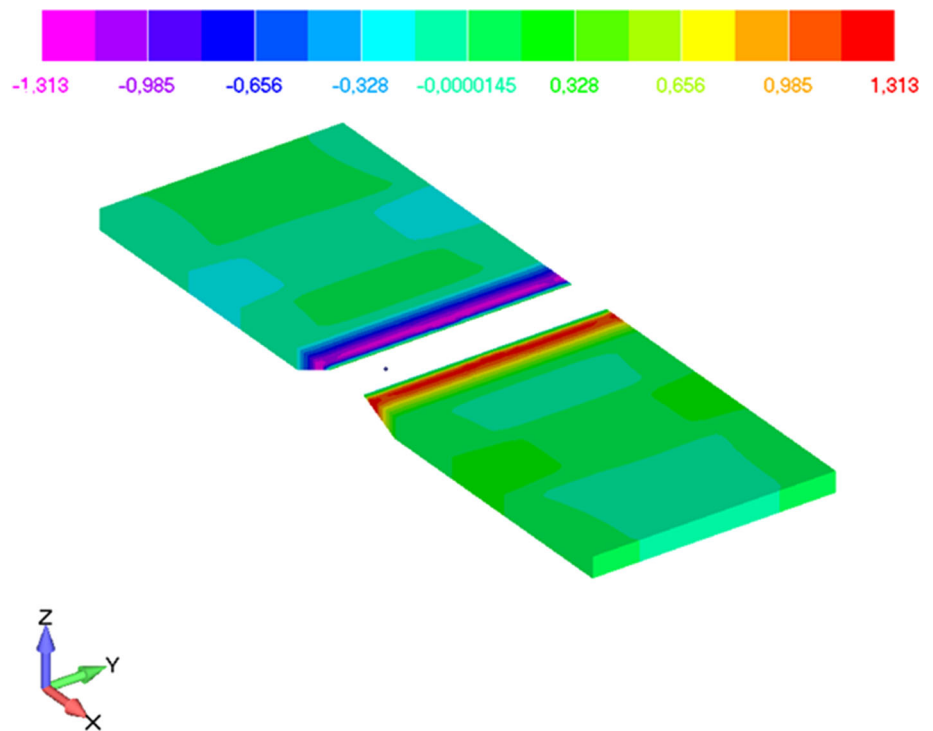


Fig. 13 Linear—shear stress-zx (MPa)



One direction about panel failure is based on the failure index considering nonlinear analysis with FPF and Tsai-Wu criteria. The nonlinear analysis is useful to obtain the results step by step defined by the user, and in composite materials the failure load is more realistic when nonlinear analysis is used. Nonlinear analysis, SOL 106 of the NASTRAN [28], was used. In this case, the option “ITER” in the

NLPPARM card was selected where the program updates the stiffness matrix at every iteration by Newton–Raphson. Also the convergence criteria were based on work error ($1E-6$ error tolerance) with the option “W.” The number of increments used was 20. Based on this analysis, Fig. 15 shows that failure occurs with 3578 N ($5112\text{ N} \times 0.7$) instead of 5112 N, by the linear analysis. So, it is very

Fig. 14 FEA (linear finite element analysis) versus test

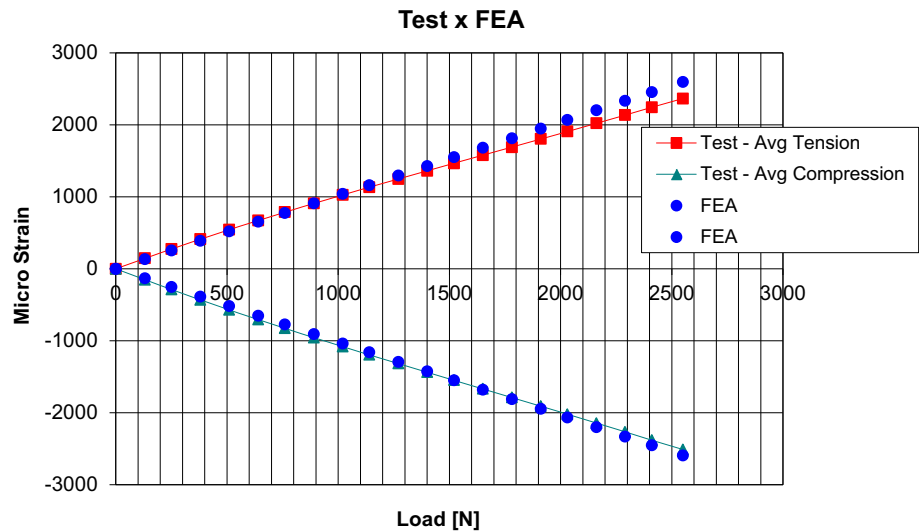
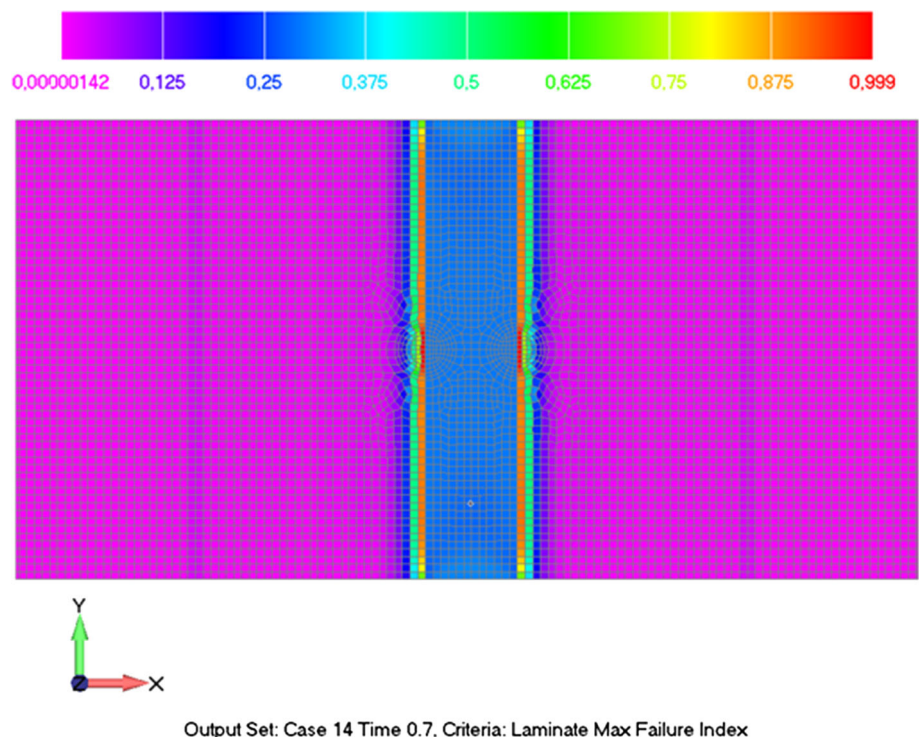


Fig. 15 Nonlinear—FPF criterion—Tsai-Wu



useful to have the test until failure to compare with design failure criteria adopted. The panel was not brought to full failure because it was used for another investigation not shown in this paper.

6 Comments and conclusions

Sandwich panels applied to primary structures are still prone to discussion due to the lack of tests to prove their reliability in new development programs. Thus, this work

contributes to new programs that are looking for new applications, considering primary structures.

Many previous works have shown the difficulty of reproducing the failure modes in sandwich structures. So, the classical literature should be validated. In this sense, the finite element model with their appropriate mechanical properties can be an option to validate the unusual failure modes. In the application example, the experimental strain results showed good correlation with the finite element method with 12.4% of the maximum error and the classical analysis showed an option to have a quick analysis in terms of the stress allowable.

For future work, it is recommended to develop new tests to investigate the specific interlaminar stresses mentioned in the literature and also environmental effects. Although there are good references on the subject, it is suggested to explore the development of a simple model, i.e., 2D element models that should deliver results as good as those of the 3D element models. Investigation where the current 2D elements can be used safely is also necessary. The justification for the use of 2D elements is the freedom and flexibility to change the properties and the core geometry, which is very useful in the early stages of new product development.

Some aspects can be explored in this paper. The use of the ramp can be an option to optimum design considering the restriction in the assembly. Also, impact behavior due to hailstone or tool drop in the transition zone can be explored with this calibrated model.

Acknowledgements The authors would like to thank those who directly or indirectly were involved with this project in special to Felipe L. Silva, Rafael S. Iwamura and Gustavo Isoni. This work was partially funded by the Brazilian Agency CNPq through Grant 300886/2013-6.

Compliance with ethical standards

Conflict of interest The authors declare that they have no conflict of interest.

References

- Polland DR et al (1997) Global cost and weight evaluation of fuselage side panel design concepts. NASA contractor report 4730, LRC
- Matsui N, Sato K (2003) Research work of the all-composite fuselage structure. In: Proceedings of 14th international conference on composite materials—ICCM14, vol 1, ID 0900, p 270
- Kupke M, Kolax M (2004) CFRP-fuselage—ensuring future competitiveness. In: SAMPE Europe conference, Paris, pp 432–437
- CMH-17 (2013) Composite materials handbook, vol 6—structural sandwich composites. SAE International Publisher, Warrendale
- Vinson JR (2005) Sandwich structures: past, present, and future. In: Thomsen OT et al (eds) Proceeding of the 7th international conference on sandwich structures. Sandwich structures 7: advancing with sandwich structures and materials, published by © 2005. Springer
- Caliri MF, Ferreira AJM, Tita V (2016) A review on plate and shell theories for laminated and sandwich structures highlighting the finite element method. *Compos Struct* 156:63–77
- D'Ottavio M, Dozio L, Vescovini R, Polit O (2016) Bending analysis of composite laminated and sandwich structures using sublaminate variable-kinematic Ritz models. *Compos Struct* 155:45–62
- Linke M, Wohlers W, Reimerdes HG (2007) Finite element for the static and stability analysis of sandwich plates. *J Sandwich Struct Mater* 9:123–142
- Wahl L, Maas S, Waldmann D, Zürbes A, Frères P (2012) Shear stresses in honeycomb sandwich plates: analytical solution, finite element method and experimental verification. *J Sandwich Struct Mater* 14(4):449–468
- Bompan BR (2017) Numerical investigation on composite sandwich panel under bending behavior. Master thesis degree, Instituto Tecnológico de Aeronáutica
- Bruhn EF (1973) Analysis and design of flight vehicle structures. Hardcover
- HyperSizer (1996–2014) Composite analysis and structural sizing software. HyperSizer documentation, Collier Research Corp
- Allen HG (1969) Analysis and design of structural sandwich panels, 1st edn. Pergamon Press, Sydney
- Burton SW, Noor AK (1995) Assessment of computational models for sandwich panels and shells. *Comput Methods Appl Mech Eng* 124:125–151
- Noor AK, Burton WS, Bert CW (1996) Computational models for sandwich panels and shells. *Appl Mech Rev* 49(3):155–199
- Bitzer T (1997) Honeycomb technology: materials, design, manufacturing, applications and testing, 1st edn. Chapman & Hall, Melbourne
- HEXCEL Composites (2000) HexWeb™ honeycomb sandwich design technology. Publication no. AGU 075b
- Niu MCY (2005) Airframe stress analysis and sizing, 2nd edn. Hong Kong Conmilit Press Ltd, Hong Kong
- Widmaier K, Arakaki FK (2007) Composite sandwich panel test proposal. Embraer technical report, DT1-CSZ-030 Rev, pp 1–24
- ESDU (2011) Engineering sciences data unit. ESDUscope, v4.9.2.0, release level 2011–07, London, UK
- ESDU 81047 (1981) Bucling flat rectangular plates. London, UK
- ESDU 87013 (1987) Elastic wrinkling of sandwich columns and beams with unbalanced laminated fibre reinforced face plates. London, UK
- ESDU 88015 (1988) Elastic wrinkling of sandwich panels with laminated fibre reinforced face plates. London, UK
- HyperSizer (2004) Composite analysis and structural sizing software. HyperSizer documentation, method: sandwich face-sheet wrinkling failure criteria. Collier Research Corp
- Ley RP, Lin W, Mbanefo U (1999) Facesheet wrinkling in sandwich structures. NASA CR-1999-208994
- Hexcel (1982) The basics of bonded sandwich construction. TSB 124
- Gutierrez AJ, Webber JPH (1980) Flexural wrinkling of honeycomb sandwich beams with laminated faces. *Int J Solids Struct* 16:645–651
- MSC Nastran 2008 r1 Quick reference guide. MSC Software Corporation, Santa Ana
- Loughlin JP (2014) Citação de referências e documentos eletrônicos. Disponível em. http://femci.gsfc.nasa.gov/hcplate/Honeycomb_Pshell.html. Acesso em 09/09/2014 as 13:33hs
- Nabarrete A, Almeida SFM, Hansen JS (2003) Sandwich-plate vibration analysis: three-layer quasi-three-dimensional finite element model. *AIAA J* 41(8):1547–1555
- Langellotti F, Isoni G (2014) Wing stub upper skin, fwd fuselage pressure bulkhead and nose landing gear bay upper cover sub-component test proposal. Embraer technical report, 550-SRP-014 Rev, pp 1–72